PHYSICAL REVIEW FLUIDS **1**, 022201(R) (2016)

Origin of critical strain amplitude in periodically sheared suspensions

Phong Pham,[1,2] Jason E. Butler,[2] and Bloen Metzger[1]
[1]*IUSTI, CNRS, UMR No. 7343, Aix-Marseille University, 13453 Marseille Cedex 13, France*
[2]*Department of Chemical Engineering, University of Florida, Gainesville, Florida 32611, USA*
(Received 1 February 2016; published 1 June 2016)

The role of solid-solid contacts on the transition between reversible and irreversible dynamics occurring in periodically sheared suspensions is investigated experimentally by modifying the particle roughness. Smoother particles lead to a larger critical strain amplitude. A geometrical model based on the assumption that colliding particles produce irreversibility is derived. The model, which considers a quasiparticle having a strain- and roughness-dependent effective volume, successfully reproduces the measured values of the critical strain amplitude as functions of the volume fraction and particle roughness.

DOI: 10.1103/PhysRevFluids.1.022201

When sheared periodically, non-Brownian particles suspended in a viscous fluid undergo a dynamical phase transition. For a given particulate volume fraction and a small enough strain amplitude, the suspension relaxes to an absorbing reversible state in which particles return to their original position after every cycle of shear. When the strain amplitude exceeds a critical value, the suspension transitions to a fluctuating state: The particles do not return to their original positions and when tracked stroboscopically at the end of each cycle of shear, the particles exhibit large fluctuations analogous to a random walk [1].

This transition caught the attention of a vast audience [1–5], owing to the assumption that the sheared suspensions are governed by reversible equations (the Stokes equations); in such a system, reversing the direction of shear would be equivalent to reversing time. Hence, suspensions were viewed as an opportunity to investigate experimentally the echo protocol, which consists of studying the evolution of a system after reversal of its dynamics [5] and addressing the emergence of macroscopic irreversibility in a system governed at the microscopic level by time-reversible laws. Within this framework, it was proposed that the irreversible motion of the particulates arises from the chaotic nature of the hydrodynamic interactions [1,6].

This long-range N-body interpretation of the problem differs from the short-range explanation put forward more recently by Corté *et al.* [7]. Without providing a clear mechanism for the physical origin of the irreversibility, Corté *et al.* modeled the suspension dynamics by convecting particles along their undisturbed streamlines until they collided, at which point the particles were displaced by a small random distance before continuing. This model, although exceedingly simple, was sufficient to explain the existence of a threshold strain amplitude and to spontaneously produce a self-organized reversible state at small strain amplitudes.

The success of the latter collision-induced model [7] is not so surprising when put in perspective with the following results: (i) Recent numerical results concluded that, in sheared suspensions, chaos arising from the long-range hydrodynamic interactions [8] or from lubrication forces [9] between particles is too weak to produce a significant irreversibility and (ii) experiments [10–14] have provided strong evidence that particle solid-solid contacts occur and significantly affect their dynamics. These studies support a growing consensus that the irreversible displacements of force-free particles in sheared suspensions are mainly driven by excluded-volume constraints.

To further assess the above paradigm and determine the physical origin of this transition, we experimentally investigated the influence of the particle roughness on the critical strain amplitude. For a given volume fraction, we find that smoother particles require a larger strain amplitude before transitioning from reversible to irreversible dynamics. A simple geometric model, based on the assumption that particle solid-solid encounters lead to irreversible displacements and which

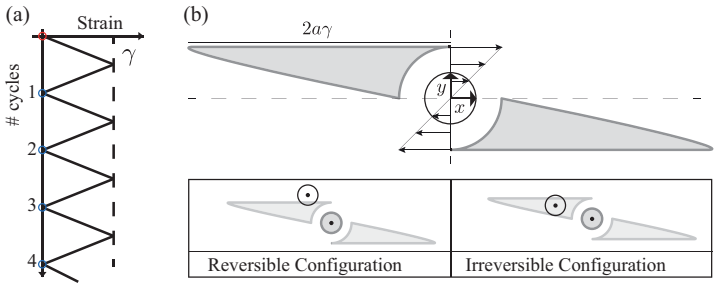

FIG. 1. (a) Schematic providing the definition of the applied strain. (b) Wing shape in two dimensions. For a given strain amplitude γ, any particle located within the gray area will eventually collide with the reference particle located at the origin.

accounts for hydrodynamic effects on the particle trajectories, is proposed and shown to predict the dependence of the critical strain amplitude on volume fraction and particle roughness.

For the sake of simplicity, we first derive the critical strain amplitude γ_c while accounting solely for the effect of the background advection flow and in a two-dimensional geometry. For a given applied strain amplitude γ [see Fig. 1(a)], any particle located within the shaded area, from now on referred to as the wings shown in Fig. 1(b), will eventually collide with the reference particle of radius a located at the origin. The area of the wings $W_{2D} = 4\gamma a^2$ is found to increase proportionally with the strain amplitude. Within the model, particles can be thought of as quasiparticles having an effective strain-dependent area $A_{\text{eff}} = \pi a^2 + 4\gamma a^2$, which is the sum of the "real" particle area plus the area of its wings.

Now consider that if N of these quasiparticles can be placed in a box of total area A without any overlap, the motion of each particle will be reversible; this condition corresponds to $NA_{\text{eff}} < \beta A$, where β denotes an order one constant. More generally, when this condition is met, we assume that the system under periodic strain can self-organize into a reversible state where no collision between the particles occurs, regardless of the initial arrangement of the particles. Conversely, if $NA_{\text{eff}} > \beta A$, the quasiparticles unavoidably overlap and produce collisions that result in irreversibility. Criticality is thus reached when $NA_{\text{eff}} = \beta A$. Using $\phi = N\pi a^2/A$, where ϕ is the real particle area fraction, the critical strain amplitude is

$$\gamma_c = \frac{\pi}{4}\left(\frac{\beta}{\phi} - 1\right). \tag{1}$$

The above simple geometrical argument predicts $\gamma_c \propto \phi^{-1}$. Despite having utilized a two-dimensional approximation, this scaling is consistent with the experimental results of Corté *et al.* [15] as well as with the scaling predicted from a three-dimensional model, which is developed next.

Using ideas similar to those above, the critical strain amplitude is now determined for fully three-dimensional suspensions while accounting for the effects of hydrodynamic interactions and short-range irreversibilities (i.e., particle roughness). The particle roughness ϵ is a dimensionless quantity that sets the distance $h = 2\epsilon a$ at which particles collide. The wing now has a more complex shape [see Fig. 2(a)]. The shape, as well as the associated volume W_{3D}, was computed numerically from predictions of the relative trajectory between two particles [16], which includes the effects of hydrodynamics and particle roughness. This Monte Carlo integration used randomly assigned positions of the particles within a box of large but fixed size together with an integration of the trajectories to identify the initial positions that result in an irreversible collision. The ratio of the number of trials that result in an irreversible collision to the total number of trials is the volume W_{3D}.

Figure 2(a) illustrates different wing shapes obtained for ($\gamma = 8, \epsilon = 10^{-3}$), ($\gamma = 6, \epsilon = 10^{-3}$), and ($\gamma = 6, \epsilon = 10^{-2}$). The wing volume is found to depend both on the strain amplitude and on particle roughness. As opposed to the former, one can anticipate the latter dependence to be nonlinear

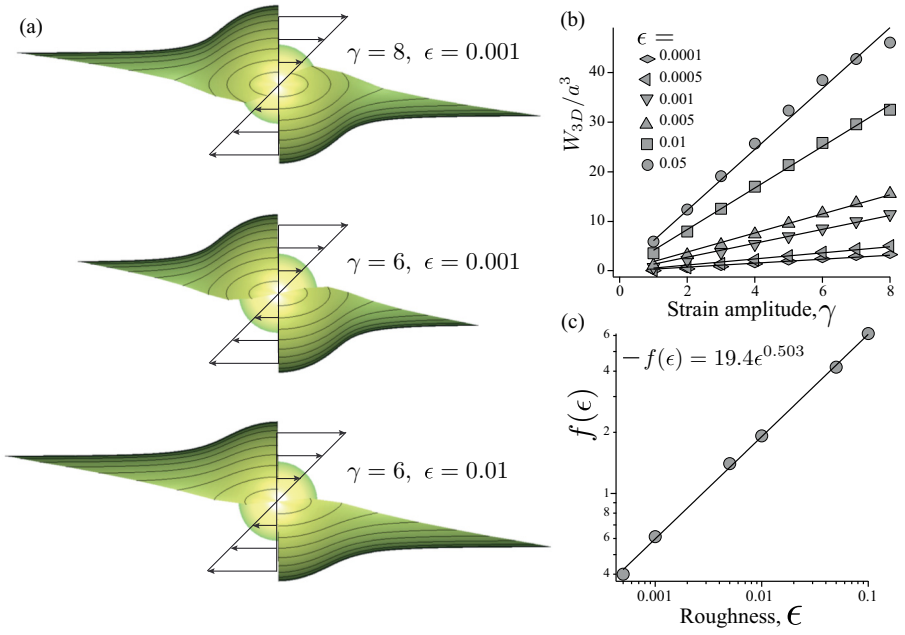

FIG. 2. (a) Wing shape in three dimensions and including the effect of hydrodynamics obtained for different strain amplitudes and particle roughness. (b) Wing volume W_{3D} versus applied strain amplitude γ for different particle roughness. The wing volume is fitted by $W_{3D}/a^3 = f(\epsilon)\gamma$. (c) The function $f(\epsilon)$ follows a power law $f(\epsilon) \propto \epsilon^{1/2}$.

as (i) the divergence of the lubrication force implies that decreasing h by a fixed amount requires an increasingly larger strain as h gets smaller and (ii) ϵ sets the distance at which particles make solid contact (when $h = 2\epsilon a$). These trends are shown in Figs. 2(b) and 2(c). Fitting the wing volume gives $W_{3D}/a^3 = f(\epsilon)\gamma$, where the function $f(\epsilon)$, as shown on Fig. 2(c), follows the power law $f(\epsilon) = 19.4\epsilon^{0.503}$, suggesting that $f(\epsilon) \propto \epsilon^{1/2}$.

For an imposed strain γ and a particle roughness ϵ, the particle effective volume in three dimensions is thus $V_{\text{eff}} = 4\pi a^3/3 + f(\epsilon)\gamma a^3$. The resulting prediction for the critical strain amplitude is

$$\gamma_c = \frac{0.22}{\epsilon^{1/2}}\left(\frac{\beta}{\phi} - 1\right). \tag{2}$$

Note that the critical strain amplitude γ_c must tend to zero at maximum packing: This sets $\beta = 0.58$ [17]. This relation also predicts that for a suspension composed of perfectly smooth spheres, i.e., $\epsilon \to 0$, the critical strain amplitude $\gamma_c \to \infty$.

To test the validity of the above relation, we performed experiments using the experimental setup in Fig. 3(a). A linear shear flow is generated by a transparent belt mounted on two vertical cylinders whose rotation is driven by a high-precision rotating stage. The fluid is a mixture of Triton X-100 (73.9 wt. %), zinc chloride (14.2 wt. %), and water (11.9 wt. %). Its composition was chosen to match both the refractive index and density of the particles, which are monodisperse spheres of poly(methyl methacrylate) with radius $a = 1$ mm. A water bath surrounding the shear cell controls the temperature at 22 °C, which is used to fine-tune the refractive index match between the particles and fluid; any adverse effects on the matching of the particle and fluid densities were small. A small amount of rhodamine 6G is added to the fluid so that, when illuminating a horizontal plane of the suspension with a (60-μm-thick) laser sheet, the particles within that plane appear as black disks as shown in Fig. 3(a) and [18].

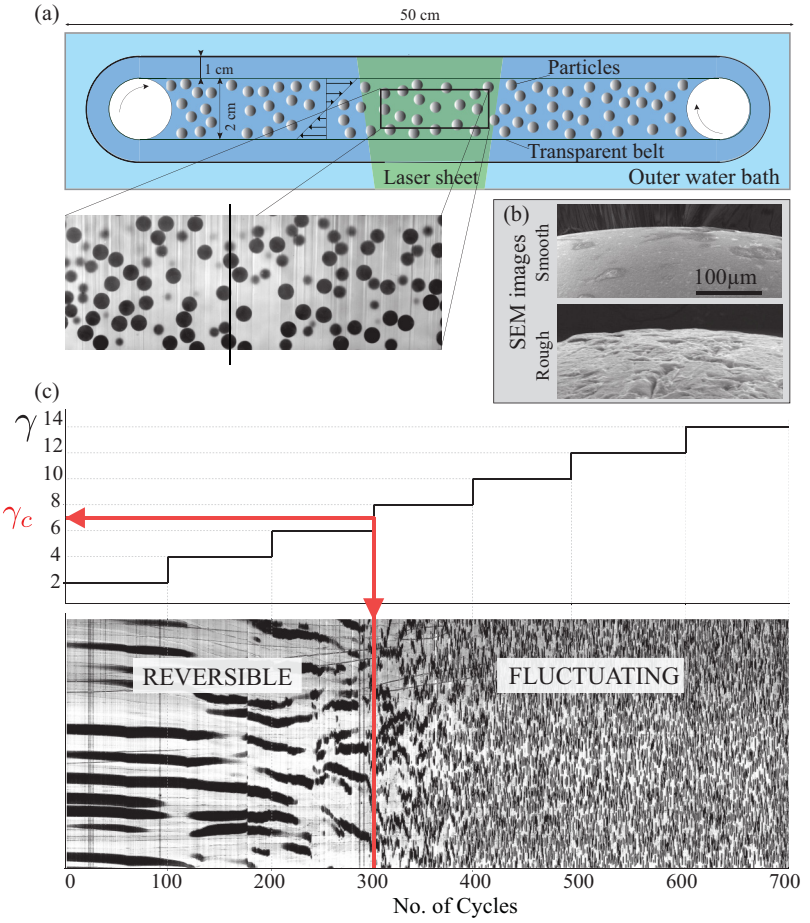

FIG. 3. (a) Top view of the experimental shear cell and a typical image of the suspension for a volume fraction $\phi = 25\%$. (b) Example images of the smooth and rough particles. (c) Determination of the critical strain amplitude. The stain amplitude is increased incrementally by steps of one strain unit. For each step, 100 cycles are performed and an image is recorded at the end of each cycle. The critical strain is directly determined from the spatiotemporal plot (red line).

The volume fraction was varied between $\phi = 25\%$ and 50% and two different batches of particles having different roughness were used. The smooth particles have a peak roughness of $\epsilon a = 1.9 \pm 1.4\ \mu$m, as was determined from averaging over multiple scanning electron microscopy images [see Fig. 3(b) for examples]. The rough particles were produced by rotating the smooth particles for 10 min at 130 rpm between two circular plates that were covered with sandpaper sheets. The resulting particles are rougher, with $\epsilon a = 5.5 \pm 3.0\ \mu$m.

Before beginning an experiment, first the suspension was spatially homogenized by preshearing it periodically at a large strain amplitude of $\gamma = 10$ for 200 cycles. Then 100 cycles were performed at each strain amplitude, as the strain amplitude was increased incrementally from 1 to 10 in steps of one strain unit as illustrated in Fig. 3(c). At the end of each cycle of oscillation, one image of the suspension was recorded and a vertical line from each image [as indicated in the example in Fig. 3(a)] was plotted in sequence. The resulting spatiotemporal plot, shown in Fig. 3(c) for $\phi = 25\%$, enables identification of the critical strain amplitude at which the particle positions become irreversible. At small strain amplitudes ($\gamma < \gamma_c$), the spatiotemporal plot shows only very small changes between each cycle, which are likely due to thermal convection and sedimentation. Conversely, at large strain

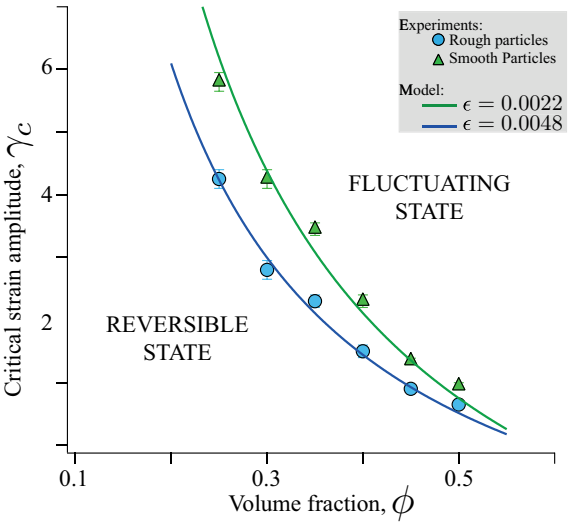

FIG. 4. Critical strain γ_c versus volume fraction ϕ, measured experimentally for the two batches of particles and comparison with the model (2): $\gamma_c = 0.22(0.58/\phi - 1)/\epsilon^{0.5}$.

amplitudes ($\gamma > \gamma_c$), the spatiotemporal plot shows that all time correlation is lost from one cycle to the next (from one vertical line of pixels to the next): The system reached its fluctuating state. The critical strain is directly determined from that spatiotemporal plot [red line in Fig. 3(c)]. After this initial coarse determination of the critical strain, the experiment was repeated with a smaller strain increment of 0.3 within the vicinity of the coarse estimate. The critical strain is thus determined within ± 0.15 strain units. Note that the critical strain amplitude characterizes the system at steady state, after oscillating a sufficient number of times to either organize the system into a reversible state if $\gamma < \gamma_c$ or into a fluctuating state if $\gamma > \gamma_c$. Therefore, the prediction of the critical strain amplitude does not depend on the initial configuration of the particles (random or presheared).

Figure 4 shows the critical strain γ_c versus volume fraction ϕ obtained for the smooth and rough particles. For rough particles, irreversibility is systematically reached at a smaller critical strain amplitude. The model (2) successfully predicts the experimental results when using values for ϵ that correspond closely to the measured values. The least-squares fit of the data, treating only ϵ as an adjustable parameter, returns $\epsilon = 0.0022$ for the smooth particles and $\epsilon = 0.0048$ for the rough particles, whereas the measurements indicate $\epsilon = 0.0019 \pm 0.0014$ and $\epsilon = 0.0055 \pm 0.003$. Note that although the model is based on the interaction of particle pairs, it predicts the critical strain surprisingly well for large volume fractions where multibody interactions might be expected to be of importance.

In conclusion, the role of solid-solid contacts on the transition occurring in periodically sheared suspensions was investigated experimentally by modifying the particle roughness. We find that changing the particle roughness has a significant impact on the amplitude of the critical strain: Smoother particles lead to a larger critical strain amplitude. We also derived a model to predict the critical strain amplitude as a function of both the volume fraction and roughness of the particles. This geometrical model is based on the assumption that irreversibility arises from solid-solid contacts between particles and considers a quasiparticle having a strain- and roughness-dependent effective volume. The interplay between the lubrication force (which diverges as the particle separation distance goes to zero) and the particle roughness (which sets the point of collision) leads to a nonlinear dependence of the critical strain amplitude on the particle roughness.

The good agreement between the model and the experimental results supports the paradigm that, in periodically sheared particulate suspensions, macroscopic reversibility is lost above a threshold strain amplitude when the particles can no longer self-organize into a configuration where time-irreversible

solid-solid contacts can be avoided. This transition occurs before (at a smaller strain) than that expected in the echo protocol. Indeed, as mentioned in the Introduction, in the pure hydrodynamic limit, when the system is fully governed by the Stokes (reversible) equations, one also expects the system to become macroscopically irreversible above a certain strain amplitude. That transition for now has been hidden by the loss of reversibility caused by solid contacts. However, according to our model, the critical strain amplitude arising from solid collisions can be increased by lowering the particle roughness. Whether it could be sufficiently increased, for instance, by using very smooth particles or a suspension of droplets, to observe macroscopic irreversibility from a loss of reversibility of the time-reversible laws constitutes an intriguing topic for further research.

We would like to thank D. Pine and E. Filippidi for discussions. P. Cervetti and S. Noel built the experimental setup. This work was supported by the National Science Foundation (Grants No. 0968313 and No. 1362060), ANR JCJC SIMI 9, and the Labex MEC Grants No. ANR-10-LABX-0092 and No. ANR-11-IDEX-0001-02.

[1] D. J. Pine, J. P. Gollub, J. F. Brady, and A. M. Leshansky, Chaos and threshold for irreversibility in sheared suspensions, Nature (London) **438**, 997 (2005).

[2] G. Düring, D. Bartolo, and J. Kurchan, Irreversibility and self-organization in hydrodynamic echo experiments, Phys. Rev. E **79**, 030101 (2009).

[3] G. I. Menon and S. Ramaswamy, Universality class of the reversible-irreversible transition in sheared suspensions, Phys. Rev. E **79**, 061108 (2009).

[4] N. Mangan, C. Reichhardt, and C. J. Olson Reichhardt, Reversible to irreversible flow transition in periodically driven vortices, Phys. Rev. Lett. **100**, 187002 (2008).

[5] R. Jeanneret and D. Bartolo, Geometrically protected reversibility in hydrodynamic Loschmidt-echo experiments, Nat. Commun. **5**, 3474 (2014).

[6] J. F. Morris, A review of microstructure in concentrated suspensions and its implications for rheology and bulk flow, Rheol. Acta **48**, 909 (2009).

[7] L. Corté, P. M. Chaikin, J. P. Gollub, and D. J. Pine, Random organization in periodically driven systems, Nat. Phys. **4**, 420 (2008).

[8] B. Metzger and J. E. Butler, Irreversibility and chaos: Role of long-range hydrodynamic interactions in sheared suspensions, Phys. Rev. E **82**, 051406 (2010).

[9] B. Metzger, P. Pham, and J. E. Butler, Irreversibility and chaos: Role of lubrication interactions in sheared suspensions, Phys. Rev. E **87**, 052304 (2013).

[10] P. A. Arp and S. G. Mason, The kinetics of flowing dispersions IX. Doublets of rigid spheres (experimental), J. Colloid Interface Sci. **61**, 44 (1977).

[11] B. Metzger and J. E. Butler, Clouds of particles in a periodic shear flow, Phys. Fluids **24**, 021703 (2012).

[12] P. Pham, B. Metzger, and J. E. Butler, Particle dispersion in sheared suspensions: Crucial role of solid-solid contacts, Phys. Fluids **27**, 051701 (2015).

[13] F. Blanc, F. Peters, and E. Lemaire, Experimental signature of the pair-trajectories of rough spheres in the shear-induced microstructure in non-colloidal suspensions, Phys. Rev. Lett. **107**, 208302 (2011).

[14] M. S. Ingber, A. A. Mammoli, P. Vorobieff, T. McCollam, and A. L. Graham, Experimental and numerical analysis of irreversibilities among particles suspended in a Couette device, J. Rheol. **50**, 99 (2006).

[15] L. Corté, S. J. Gerbode, W. Man, and D. J. Pine, Self-organized criticality in sheared suspensions, Phys. Rev. Lett. **103**, 248301 (2009).

[16] F. R. da Cunha and E. J. Hinch, Shear-induced dispersion in a dilute suspension of rough spheres, J. Fluid Mech. **309**, 211 (1996).

[17] F. Boyer, E. Guazzelli, and O. Pouliquen, Unifying suspension and granular rheology, Phys. Rev. Lett. **107**, 188301 (2011).

[18] See Supplemental Material at http://link.aps.org/supplemental/10.1103/PhysRevFluids.1.022201 for a video showing sequential images of the particles at the end of each cycle of shear along with the corresponding spatiotemporal plots.